RSC Advances

PAPER

View Article Online
View Journal | View Issue

Cite this: *RSC Adv.*, 2016, **6**, 47509

Electrochemical treatment of mature landfill leachate using Ti/RuO_2–IrO_2 and Al electrode: optimization and mechanism

Juan Li,[ab] Zhao-hui Yang,*[ab] Hai-yin Xu,[ab] Pei-pei Song,[ab] Jing Huang,[ab] Rui Xu,[ab] Yi-jie Zhang[ab] and Yan Zhou[ab]

Received 26th February 2016
Accepted 6th May 2016

DOI: 10.1039/c6ra05080h

www.rsc.org/advances

Today, improving the elimination of refractory pollutants in landfill leachate through electrochemical oxidation technology has attracted considerable attention. In this study, a combination of anodic oxidation and cathodic coagulation process using Ti/RuO_2–IrO_2 and Al electrodes, was adopted to treat the mature landfill leachate with a very low biodegradability ratio (BOD_5/COD) of 0.12. The effects of current density, pH, and the chloride ion concentration on the removal of chemical oxygen demand (COD) and ammonia nitrogen (NH_3–N) were investigated by response surface methodology (RSM). The optimum condition of 83.7% COD and 100% NH_3–N removal was achieved with a current density of 0.1 A cm^{-2} and a pH of 6.37, the chloride ion concentration 6.5 g L^{-1}, and an electrolytic time of 150 min. In addition, heavy metals were partly removed. A main degradation mechanism of the pollutants, including oxidation, coagulation and precipitation, was elucidated by gas chromatography-mass spectrometry (GC-MS), environmental scanning electron microscopy coupled with energy dispersive spectrometer (ESEM/EDS) and Fourier transform infrared spectroscopy (FT-IR) analysis of organic components in landfill leachate and sludge generated at the cathode. These results indicated that the electrochemical processes could be a convenient and efficient method for the treatment of landfill leachate.

1. Introduction

Rapid economic development and population growth followed by inadequate infrastructure, expertise, and land scarcity have resulted in an increase in the amount of municipal solid waste (MSW).[1,2] Even if there are many options for municipal solid waste management, sanitary landfill remains the most common and desirable management strategy due to low cost, simple procedures and landscape restoring effect on holes from mineral working.[3] But the secondary pollution of concomitant landfill leachate has become one of the most critical environmental issues.[4] Generally, landfill leachate can be considered as a complex and high-polluting strength wastewater that possesses suspended solids, nitrogen compounds, various types of organic compounds and heavy metals.[5] The composition and concentration are mainly dependent on the type of waste and the age of the landfill.[6] Among them, the high concentration of chemical oxygen demand (COD) and ammonia nitrogen (NH_3–N) are the key factors.[7] If without any appropriate treatment, landfill leachate contributes to severe pollution of the receiving water bodies, and likewise imparts an adverse impact on the ecosystem and public health.[8] Thus, environmental regulations require that the leachate must be pretreated on site to meet the standards for its discharge into the sewer or surface water.

Because of recalcitrant NH_3–N and relatively low five-day biological oxygen demand (BOD_5)/chemical oxygen demand (COD) ratio, mature landfill leachate (>10 years)[9] can not be treated by conventional biological treatment, such as aerobic and anaerobic biological degradation.[10] However, the electrochemical oxidation process with high effectiveness, environmental compatibility and easy in operation has been shown as a promising alternative for NH_3–N removal.[11] In the electrochemical oxidation,[12] employing different types of anode materials plays a dominant role, and substantially influences both reaction selectivity and efficiency,[13,14] such as Ti, PbO_2/Ti, RuO_2, Fe, Al, and boron-doped diamond (BDD), *etc.*[15] Among the various anodes used, RuO_2 and IrO_2 coated Ti anode (Ti/RuO_2–IrO_2) stands out, which has been utilized widely with well-proven advantages.[16] It possesses high stability and catalytic activity, not only for chlorine evolution, but also for oxygen evolution. Several authors have applied Ti/RuO_2–IrO_2 electrode to the treatment of landfill leachate.[3] Usually, cathode is protected against corrosion in the electrooxidation technology. Except for a carrier of the electronic, it does not have substantial effect. On the contrary, taking advantage of the cathode corrosion and investigating the effect in the solution have a certain

---

[a] *College of Environmental Science and Engineering, Hunan University, Changsha 410082, PR China. E-mail: yzh@hnu.edu.cn; Fax: +86 0731 88822829; Tel: +86 0731 88822829*

[b] *Key Laboratory of Environmental Biology and Pollution Control (Hunan University), Ministry of Education, Changsha 410082, PR China*

significance. As the third most abundant element in the earth crust, aluminum and its alloys are recognized to be one of the most suitable metals for future hydrogen production, energy storage and conversion.[17,18] Moreover, aluminium as the cathode can produce hydroxide at the expense of sacrificial aluminum, which has a promoting coagulation effect on pollutant removal.[17] In consequence, we can construct electro-oxidation and coagulation into a system to further improve the efficiency of processing, which has not been studied yet. When anodic oxidation is combined with the cathodic coagulation, structure of reaction tank can be optimized. Compared with the pure electrochemical oxidation, the removal rate of pollutants is improved significantly.

In this study, mature landfill leachate was treated by the combination of electrooxidation–coagulation processes using $Ti/RuO_2–IrO_2$ anode and Al cathode. The main objectives can be divided into three aspects. Firstly, the effects of various operating variables *e.g.* electrolytic time, electrode gap, current intensity, pH and initial concentration of chloride ions on COD, NH_3–N, colour and heavy metals removal were investigated. In parallel, response surface methodology (RSM) was considered to be an effective means to evaluate their interactions and determine the optimum operational conditions.[10] Secondly, some associated mechanisms were presented, regarding oxidation and coagulation that occurred in the electrode/solution boundary. Finally, energy consumption was used to examine its performance in the electrochemical process.

2. Materials and methods

2.1 Materials

The used leachate was sampled from Heimifeng Landfill located in Changsha (China). It has been running since 2003. This plant covers about 174 ha surface and treats more than 3000 tons solid waste daily. Table 1 provided a general physicochemical characteristics of the raw leachate in accordance with the standard methods.[19] As could be seen, the raw leachate presented with a black color, which was associated with a high organic pollutant charge, high ammonia nitrogen content, and a low BOD_5/COD (0.12) ratio. It could be categorized as mature landfill leachate because of low biodegradability. There was a high concentration of chlorine, sodium and potassium within this leachate, which led to a high conductivity of 12.62 mS cm^{-1}, permitting the application of electrochemical process. It also contained a relatively low concentration of toxic heavy metals, which tended to accumulate in the biological organisms.

Table 1 The characteristics of leachate samples

Parameters	Unit	Range	Average
pH	—	7.80–8.28	8.04
Conductivity	mS cm^{-1}	12.05–13.08	12.62
Cl^-	mg L^{-1}	2300–2800	2500
BOD_5	mg L^{-1}	440–520	480
COD	mg L^{-1}	3640–4296	3968
BOD_5/COD	—	0.10–0.14	0.12
NH_3–N	mg L^{-1}	1840–2042	2000
Sodium	g L^{-1}	3.528–3.800	3.664
Potassium	g L^{-1}	1.264–1.386	1.325

2.2 Experimental procedures

The experimental setup was shown in Fig. 1. In this study, electrodes with surface area of 35 cm^2 (=anode: $Ti/RuO_2–IrO_2$; cathode: Al), were placed vertically and parallel to each other in the electrolytic reactor containing 500 mL of leachate sample. A precision digital direct current power supply (DC, 0–32 V, 0–5 A) was used to provide the desired current. Initial pH was adjusted with concentrated nitric acid or sodium hydroxide. Solid sodium chloride (NaCl), as electrolyte was added before each experiment. The reactor was placed on a magnetic stirring block at a maintained speed of 200 rpm, in order to keep its contents well mixed during the experiment. Besides, all experiments were conducted at room temperature and atmospheric pressure. After each run, the sample was settle down for 20 min and the supernatant was taken to make analysis.

2.3 RSM experimental design

Response surface methodology (RSM) was an experimental technique used for predicting and modeling complicated relationship between independent factors and one or more responses.[20] Additionally, it could reduce the number of runs in comparison with the orthogonal experiment method. Central composite design (CCD), a branch of RSM, was appropriate to fit a quadratic model, as well as to select optimal condition of variables and predict the best value of responses.[21] Operating between the responses of the corresponding coded values and the different process variables, the response model might be expressed by a second-degree polynomial equation as illustrated in eqn (1):

$$y = b_o + \sum_{i=1}^{m} b_i x_i + \sum_{i<j}^{m} b_{ij} x_i x_j + \sum_{i=1}^{m} b_{ii} x_i^2 \quad (1)$$

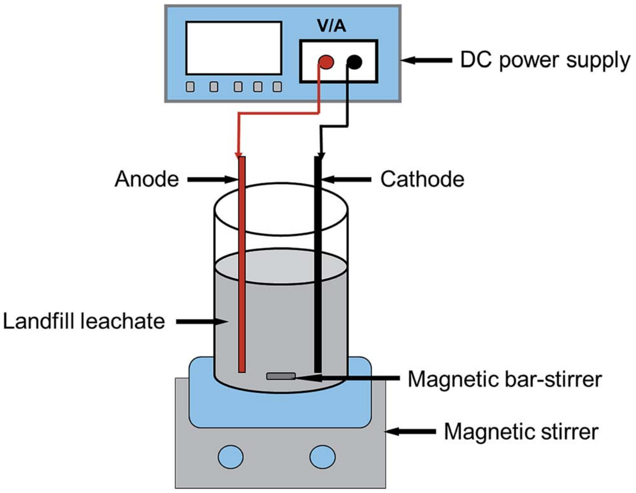

Fig. 1 Schematic of a simplified reactor that represented the design of electrochemical reactor.

where y is the response variable, b_o is a constant, b_i, b_{ii}, and b_{ij} are the linear, quadratic, and interaction coefficients, respectively. x_i and x_j are independent variables ($i \neq j$).

On the basis of the single factor test results, three independent variables (current density (x_1), pH (x_2) and the chloride ion concentration (x_3)) and two responses (COD and NH_3–N removal) were investigated in this experiment. The practical design parameters and their levels were presented in Table 2, with the help of the Design Expert software (Version 8.0.6, Stat-Ease Inc, Minneapolis, MN). Then, it was also used for handle of the experimental data to obtain the equations and analysis of variance (ANOVA).[10] The test of statistical significance must be based on the total error criteria with a confidence level of 95.0% ($p < 0.05$). R^2, which ranged from 0 to 1, was used to express the fit quality of the polynomial model equation. When R^2 value closer to 1, it meaned the model was more accurate. Three dimensional (3D) response surface plots were constructed from the developed models in order to study the individual and interactive effect of the process variables on the responses. And all response surface plots have clear peaks, meaning that the optimum conditions were located to find out maximum values of the responses.

2.4 Analysis and calculations

The instruments used to measure conductivity and pH were conductivity meter (DDS-11A, Shanghai) and pH meter (HI 98184, HANNA, Italy), respectively. Levels of chloridion was measured using silver nitrate titration method according to the standard methods.[19] Used for the performance evaluation, COD was determined by a fast digestion-titration method based on the potassium dichromate, and NH_3–N was determined spectrophotometrically using the Nesslerisation method at an absorbance of 425 nm. The concentration of heavy metals in the solution were analyzed by inductively coupled plasma-atomic emission spectrometry (ICP-AES, PS-6, Barid Company, US). Organic composition was determined by gas chromatography-mass spectrometry equipment (GC/MS, Model QP-2010, Shimadzu, Japan). Environmental scanning electron microscopy (ESEM) coupled with energy dispersive spectrometer (EDS) (Quanta 200 FEG, FEI, US) and Fourier transform infrared spectroscopy (FTIR-8400S, IRprestige-21) were chosen to characterize the sludge generated in experiment.

The percentage removal of pollutant in the aqueous solution was calculated by using eqn (2):

$$\text{Removal rate} = \frac{C_o - C_e}{C_o} \times 100\% \tag{2}$$

where C_o and C_e are the initial and final concentration, respectively.

Electric energy per mass, E_{EM} (kW h kg^{-1}), was proposed by Bolton to judge economic feasibility, whether was suitable for large scale application.[22] It was defined as the electric energy in kilowatt hour (kW h) required to degrade a kilogram of a specific pollutant in contaminated water, as described by eqn (3):

$$E_{EM} = \frac{UIt}{(C_o - C_e)V} \tag{3}$$

where E_{EM} is the electrical energy consumption (kW h kg^{-1}), U is the potential (V), I is the current (A), t is the time (h), V is the volume of the solution treated (L), C_o (mg L^{-1}) and C_e (mg L^{-1}) are the concentrations of pollutants before and after electrochemical process.

3. Results and discussion

3.1 Factors influencing COD and NH_3–N removal

As exemplified by Fig. 2(a), Al cathode showed higher rates for COD and NH_3–N removal than that of Ti/RuO_2–IrO_2. This could be explained by the fact that chemical dissolution of aluminum occurred when the aluminum was polarized cathodically. Al cathode transferred higher numbers of Al^{3+} into the solution and they produced a higher amount of sludge. And these sludge had a coagulation effect on pollutants in the landfill leachate. The phenomenon also referred to as "chemical dissolution" or "cathodic corrosion",[17] which was contribute to color removal meanwhile and 100% efficiency were observed in Fig. 2(b). From the above, our subsequent experiment focused on Ti/RuO_2–IrO_2 anode and Al cathode.

On the other hand, Fig. 2(a) showed the influence of reaction time on the COD and NH_3–N removal rate when it was varied from 0 to 180 min. Electrolytic time had a positive effect on mineralization and decolorization of leachate. It was noted that the maximum COD and NH_3–N removal was obtained with an optimal electrolytic time of about 150 min. When the allowed reaction time longer than 150 min, the removal rate were not further improved considerably.

In a parallel-plate monopolar reactor, the electrical field and conductivity could be controlled by varying electrode gap.[23] In order to investigate the effect of inter-electrode distance on the efficiency of the process, the reactor was arranged such that

Table 2 Experimental range and levels of the independent variables

		Range and level				
Variables		−1.682	−1	0	1	1.682
Current density (A cm^{-2})	x_1	0.04	0.05	0.07	0.09	0.1
pH	x_2	5.00	5.81	7.00	8.19	9.00
The chloride ion concentration (g L^{-1})	x_3	2.50	3.31	4.50	5.60	6.50

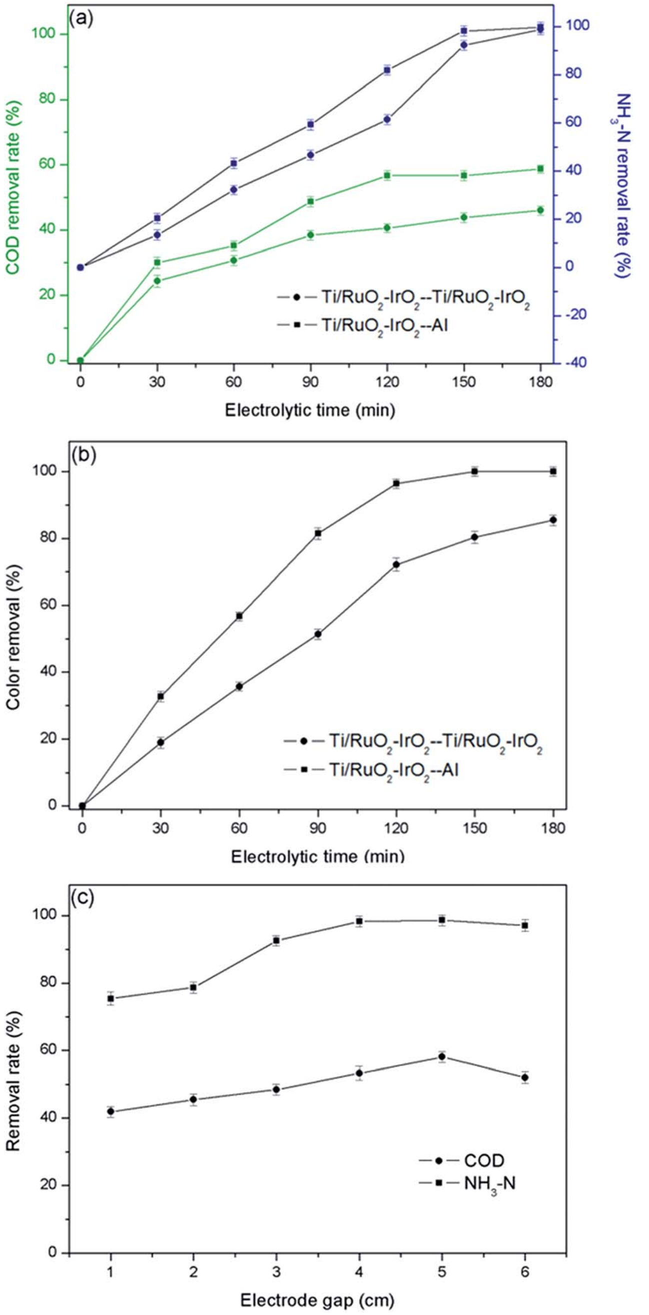

Fig. 2 Effects of electrode materials, electrolytic time on COD, NH_3–N (a) and color (b) removal, and effect of electrode gap on COD and NH_3–N removal (c).

electrodes were positioned at 1 cm to 6 cm. Fig. 2(c) showed the COD and NH_3–N removal rates obtained from different distances. We could conclude that COD and NH_3–N removal rates increased with an increase in electrode gap, until it was 5 cm. This might be related to diffusion limitations at small gap system. Subsequently, the removal rates was decreased. This suggested that the resistivity of the solution increased and it will reduce the mass transfer efficiency. Hence, the recommended gap in our experiment was 5 cm, which was kept constant in all experiments.

3.2 RSM design

3.2.1 Quadratic model. According to the RSM results in regard to the response variables of COD and NH_3–N removal, which were acquired from 20 groups of experiments with the help of Design-Expert software, the final optimum fit model equations were obtained as follows:

COD removal rate:

$$y_1 = 52.91 + 9.40x_1 - 9.46x_2 - 2.81x_3 + 0.33x_1x_2 + 1.46x_1x_3 + 1.23x_2x_3 + 3.68{x_1}^2 + 0.84{x_2}^2 + 0.33{x_3}^2 \quad (4)$$

NH_3–N removal rate:

$$y_2 = 76.74 + 18.33x_1 + 11.54x_2 + 1.44x_3 + 3.62x_1x_2 + 3.67x_1x_3 - 2.70x_2x_3 - 3.95{x_1}^2 - 5.03{x_2}^2 - 0.29{x_3}^2 \quad (5)$$

On the basis of the experimental values, statistical testing was carried out using Fisher's test for ANOVA of regression parameters in quadratic model. Results were listed in Table 3 and indicated the second-order equation fitted well. Because the Prob > F of model was less than 0.05, and total determination coefficient R^2 of COD and NH_3–N reached 0.9535, 0.9749, respectively.

3.2.2 Interaction between variables. Fig. 3(a) and (d) clearly represented the effects of current density (x_1) and pH (x_2) on the COD and NH_3–N removal, while the chloride ion concentration (x_3) was fixed. It indicated that the COD and NH_3–N removal rates increased significantly when the current density was increased upto 0.1 A cm^{-2}. Thereafter, there was a negligible effect on removal rates of COD and NH_3–N. This was attributed to the higher formation of hydroxyl radicals species ($OH^\bullet$) that was controlled by the applied current during electrolysis. $OH^\bullet$ had the strong positive effects on the organic matters presented in the landfill leachate, thus the removal rates were increased.[16] pH was a very important parameter for electrochemical degradation of COD and NH_3–N in landfill leachate. Under the acidic condition, the removal rate of COD was relatively high. In neutral or alkaline solution, it was more suitable for removal of NH_3–N. The reasons could be as follows. Firstly, the amounts of $OH^\bullet$ were large at low pH, which could accelerate the mineralization of COD. Besides, small molecule organic matters were easier to be eliminated than NH_3–N with larger radius. Secondly, in high pH, organic matters were in stable non-dissociation state and hard to be removed. Nevertheless, the proportion of ammonia in the form of $NH_3 \cdot H_2O$ which could be stripped out of solution was improved.[24]

Fig. 3(b) showed COD and NH_3–N removal with the variation of current density (x_1) and the chloride ion concentration (x_3), as well as the interaction between them. With current density at low levels, COD removal was higher with the decrease of the chloride ion concentration owning to the decrease of oxidation capacity of anode in high NaCl dosage. On the contrary, with current density at high levels, the higher removal of COD was obtained at high chlorine ion concentration. That was probably because more active free chlorine could be generated by increasing the current density and chloride concentration simultaneously, according to Czarnetzki and Janssen

Table 3 ANOVA results for response surface quadratic model analysis of variance

	Source	Sum of squares	Degree of freedom	Mean square	F-Value	Prob > F	
COD removal (%)	Model	2186.53	9	242.95	22.78	<0.0001	Significant
	x_1	845.93	1	845.93	79.32	<0.0001	
	x_2	1074.18	1	1074.18	100.72	<0.0001	
	x_3	0.49	1	0.49	0.046	0.8343	
	x_1x_2	22.51	1	22.51	2.11	0.1769	
	x_1x_3	99.55	1	99.55	9.33	0.0121	
	x_2x_3	13.42	1	13.42	1.26	0.2883	
	Residual	106.65	10	10.67			
	Lack of fit	87.06	5	17.41	4.44	0.0637	Not significant
	Pure error	19.60	5	3.92			
S.D. = 3.27, PRESS = 690.55, $R^2 = 0.9535$, $R_{adj}{}^2 = 0.9116$, Adeq precision = 16.430.							
NH_3–N removal (%)	Model	7246.63	9	805.18	43.19	<0.0001	Significant
	x_1	4586.53	1	4586.53	246.04	<0.0001	
	x_2	1818.37	1	1818.37	97.55	<0.0001	
	x_3	28.50	1	28.50	1.53	0.2445	
	x_1x_2	104.84	1	104.84	5.62	0.0392	
	x_1x_3	107.75	1	107.75	5.78	0.0370	
	x_2x_3	58.54	1	58.54	3.14	0.1068	
	Residual	186.41	10	18.64			
	Lack of fit	180.50	5	36.10	30.55	0.0009	Significant
	Pure error	5.91	5	1.18			
S.D. = 4.32, PRESS = 1533.46, $R^2 = 0.9749$, $R_{adj}{}^2 = 0.9524$, Adeq precision = 22.476.							

reported.[25] It was obviously seen that the NH_3–N removal exhibit the same tendency, as shown in the Fig. 3(e).

Fig. 3(c) presented the interaction between pH (x_2) and the chloride ion concentration (x_3) and their effects on the COD and NH_3–N removal. Increasing the chloride ion concentration (x_3) to 4.5 g L^{-1} at a range from 5 to 7 for the pH (x_2) decreased COD removal rate, whereas further increase in the chloride ion concentration (x_3) made the removal rate of COD remain unchanged. From 7 to 9 of the pH (x_2), the chloride ion concentration increasing was usually accompanied a moderate but significant acceleration of treatment rate in terms of COD removal. Previous studies showed similar results of various electrolytes like NaCl, KCl, $NaNO_3$, $NaSO_4$, *etc.*[26] But, due to low cost and easy availability, NaCl was worthy of being selected as the best electrolyte.[27] For NH_3–N removal shown in Fig. 3(f), there was the just the opposite with the COD removal results.

As can be seen in Fig. 3, average removal rate of NH_3–N were higher than COD during the electrolysis, which was agreement with the reports by Chiang[28] and Feki *et al.*[29] During the electrochemical process, both COD and NH_3–N could be removed simultaneously and there would be a competition between them yet. According to the report by Deng and Englehardt, the rule of competition between removal of COD and NH_3–N seemed to be that the removal of NH_3–N was greater than that of COD when indirect oxidation was prevalent, whereas COD removal took priority under direct anodic oxidation.[30]

3.2.3 Optimization of the electrolysis process. According to RSM, the optimized conditions occurred at current density 0.1 A cm^{-2}, pH 6.37, the chloride ion concentration 6.5 g L^{-1}, reaction time 150 min and electrode gap 5 cm, which should result in COD removal of 84.26% and NH_3–N removal of 100%. In order to confirm the accuracy and reliability of the predicted value, an experiment was then conducted. Table 4 showed that the experimental values were fitted well with the predicted ones, and COD and NH_3–N removal rates were 83.93% and 100% respectively. It also confirmed that RSM was a powerful tool for optimizing the operational conditions of electrochemical experiment with great accuracy. Comparing the performance of the other cathode material systems in the literatures,[31–37] which showed in Table 5, we could reasonably conclude that Al was more superior to COD and NH_3–N removal carried out at less time.

Besides enhanced the treatment efficiency of COD and NH_3–N, this procedure also had the potential to eliminate possible heavy metals, like chromium, zinc and part of the aluminum introduced during the cathodic corrosion process. A number of studies demonstrated the natural attenuation of heavy metals within a landfill. However, there were many varieties of heavy metals in landfill leachate, such as Fe, B, Al, Ni, Zn, Cr, As, Pb, Co, Se, and Cu, the concentration of which was relatively low, as shown in Table 6. After 150 min electrolytic time on the optimal conditions, the removal rates of heavy metals comparing with the initial concentrations were 99.60%, 28.57%, 100.00%, 93.33%, 16.67%, 33.33%, 95.00%, 90.00%, 100.00%, 80.00%, and 100.00%, respectively. These results could be explained with respect to cathode corrosion, where sludge provided functional groups (hydroxyl) on the large surface to remove heavy metals through electrostatic absorption or frequent coagulation.[38]

3.3 Mechanism analysis

In the following subsections, a detailed description of these mechanisms that responsible for pollutants removal during the

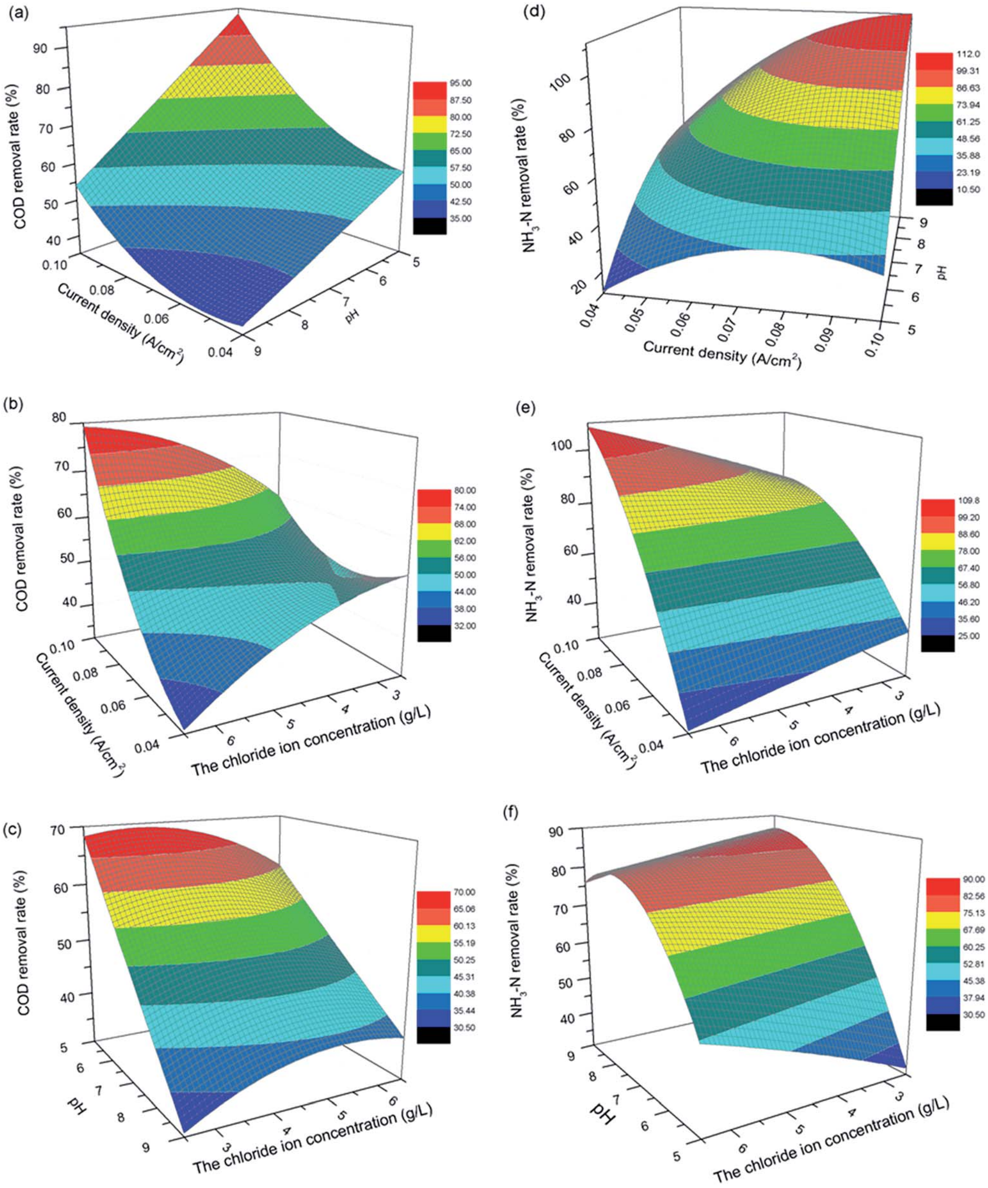

Fig. 3 3D surface plots for COD (a–c) and NH_3–N (d–f) removal efficiency as a function of two independent variables (other variables were held at their respective center levels).

Table 4 Optimum conditions found by design expert and verification for COD and NH_3–N removals

Response	Current density (A cm^{-2})	pH	The chloride ion concentration (g L^{-1})	Removal rate (%)		Error	Desirability
				Predicted	Observed		
COD	0.10	6.37	6.50	84.26	83.93	0.33	87.2%
NH_3–N	0.10	6.37	6.50	100	100	0.00	87.2%

combination of electrooxidation and coagulation processes of landfill leachate, was going to be carried out by GC-MS, ESEM/EDS and FT-IR analysis of organic components in landfill leachate and sludge generated in cathode.

3.3.1 Analysis of organic compounds in landfill leachate. In order to gain insight into the organics in the leachate before and after electrochemical experiment, leachate contents in the influent and effluent of the electrochemical reactor were analyzed by the gas chromatography-mass spectrometry system (GC-MS).[39] There were 109 kinds of organic pollutants detected in the original landfill leachate, whose match percent was not less than 85%, including acids, esters, cyclic ketone, the long-

Table 5 The research results previously reported for the degradation of leachates by electrochemical oxidation under the different cathode[a]

Anode	Cathode	Current density (A cm^{-2})	pH	Reaction time (min)	Initial COD concentration (mg L^{-1})	COD removal (%)	Initial NH_3–N concentration (mg L^{-1})	NH_3–N removal (%)	References
Ti/RuO_2–IrO_2	Ti	0.116	8.25	180	1855	73	1060	49	31
Ti/RuO_2–IrO_2	Ti/RuO_2–IrO_2	0.200	8.60	240	3973	87.4	1726.6	NS	32
Ti/RuO_2–IrO_2	Stainless steel	0.060	8.40	180	2091	20.2	2531	57.7	33
Ti/RuO_2–IrO_2	Stainless steel	0.244	7.60	41.78	1375	54.99	1200	71.07	34
Ti/RuO_2–IrO_2	Zr	0.032	3.00	240	2960	65	14	NS	35
Ti/RuO_2–IrO_2	Cu/Zn	0.025	7.80	360	NA	NA	60	95.98	36 and 37
Ti/RuO_2–IrO_2	Fe	0.020	7.00	180	NA	NA	100	87	37

[a] NA-not applied; NS-not specified.

Table 6 Heavy metals removal from landfill leachate using Ti/RuO_2–IrO_2 and Al electrode in optimum conditions

Species	Initial concentration (mg L^{-1})	Final concentration (mg L^{-1})	Removal rate (%)
Fe	14.90	0.06	99.60
B	2.80	2.00	28.27
Al	0.70	0.00	100.00
Ni	0.30	0.02	93.33
Zn	0.30	0.25	16.67
Cr	0.30	0.20	33.33
As	0.20	0.01	95.00
Pb	0.10	0.01	90.00
Co	0.08	0.00	100.00
Se	0.05	0.01	80.00
Cu	0.02	0.00	100.00

chain hydrocarbons, *etc.* As shown in Fig. 4, it was evident that the species and mass percentage of organic compounds in landfill leachate were found to have considerably declined during electrochemical process. However, some new compounds were detected in the effluent of the electrochemical reactor. These results implied that it produced refractory matter which were difficult to remove absolutely, when strong oxidant convert macromolecular organic to small molecule organic.[40]

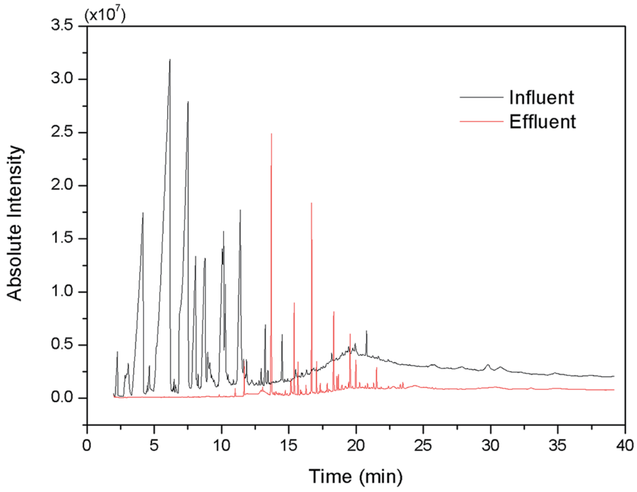

Fig. 4 GC-MS analysis of leachate before and after electrochemical experiment.

3.3.2 Characterization of sludge. Knowing the crystalline structures and composition of sludge that produced from aluminum cathode would provide valuable information, regarding the fundamental mechanisms of pollutants removal. To evaluate the structural features, ESEM image and EDS spectra of particles sludge were performed. As illustrated in Fig. 5(a), ESEM image displayed the presence on the surface of mostly amorphous or ultrafine particular structure at micrometer size. In Fig. 5(b), the detected elements analysis by EDS indicated that the surface of these particles was coated with a layer of contaminant, most likely C, O, and Al species. These results confirmed the existence of cathode corrosion process and it was helpful to remove pollutants presenced in the solution.

Fig. 5(c) showed FT-IR spectra of sludge in the 500–4000 cm^{-1} range, which revealed formation of new species in electrochemical process. From curve, apparition of a peak at 528.5 cm^{-1}, 657.73 cm^{-1} at 1377.17 cm^{-1} were ascribed to Al–OH, Al–O and Al–H bending, which were characteristic of $Al(OH)_3$ or $Al(OH)_4{}^-$.[41] As a coagulant, hydroxides of aluminum could be considered the responsible constituent of heavy metals removal. Additionally, peaks 1419.61 cm^{-1} and 1637.56 cm^{-1} were also observed corresponding to –COOH stretching and H–O–H bending respectively. C–H vibration in aromatic structures was represented by the band at 3051.39 cm^{-1}.[42] These indicated the part of organic pollutants in landfill leachate might be adsorbed on coagulant surface. It also had absorbance bands with maxima at 3442.94 cm^{-1} representing O–H stretching of hydroxyl groups from hydrogen bonding.[43] Thus, all of these showed that coagulation process duo to the cathodic corrosion were successfully remove some pollutants.

3.3.3 Reaction mechanism. Fig. 6 showed the reaction mechanism responsible for the removal of pollutants. As the reaction progresses, the evolution of pH and the chloride ion concentration (Fig. 7) were found to be inter-related, which can be interpreted in terms of the electrochemical and the chemical reactions. As follows, the species within the solution participated in the reactions in a different manner.

In anode: Pollutions removal in the presence of electrolyte (NaCl) were carried out in two ways *viz.*:

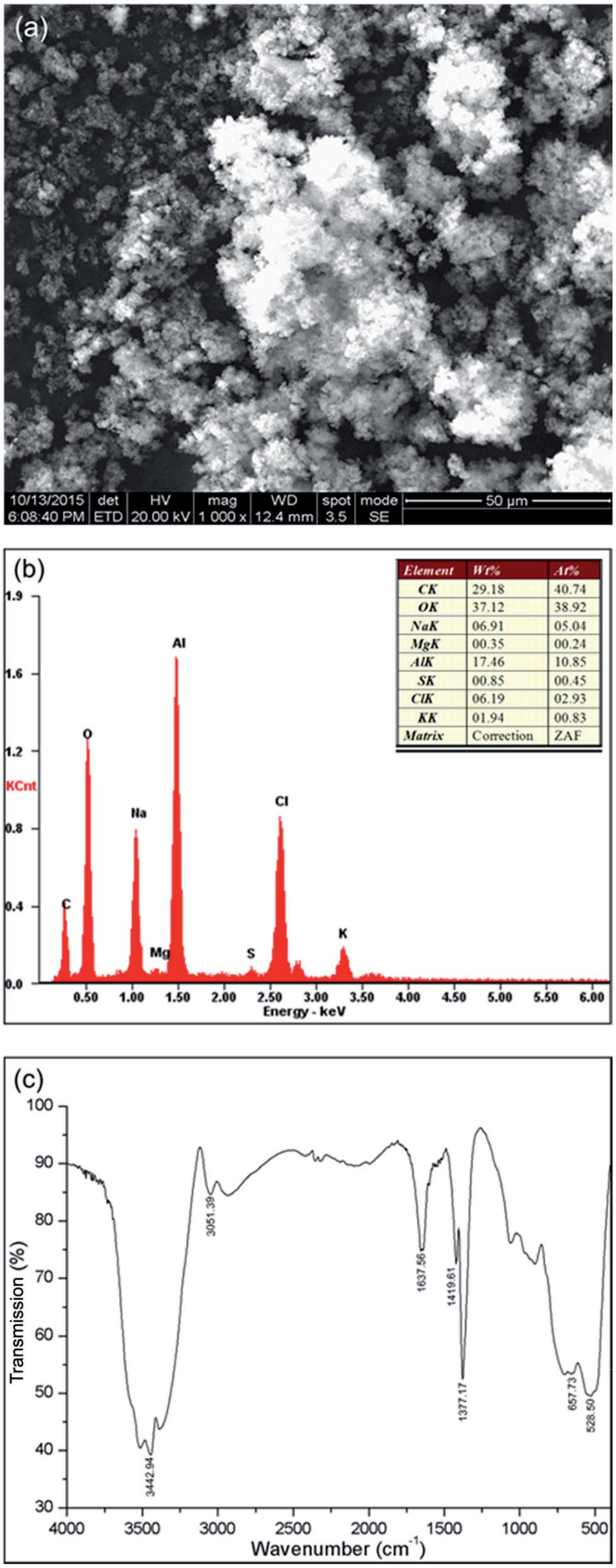

Element	Wt%	At%
CK	29.18	40.74
OK	37.12	38.92
NaK	06.91	05.04
MgK	00.35	00.24
AlK	17.46	10.85
SK	00.85	00.45
ClK	06.19	02.93
KK	01.94	00.83
Matrix	Correction	ZAF

Fig. 5 (a) ESEM image, (b) EDS spectra and (c) FT-IR spectra of the sludge generated in the electrochemical process.

(i) Direct oxidation: On Ti/RuO$_2$–IrO$_2$ anode, almost complete mineralization of some organic matter with very high current density was obtained, which occurred through direct electron transfer in the potential region. In addition, hydroxyl radicals or other reactive species were generated from water electrolysis owing to the high overpotential for oxygen production, and participated in the electrochemical oxidation at the anode surface.[39] They could promote the oxidation/reduction reactions of the organic pollutants, contained in the electrochemical cell, which improved the removal of large recalcitrant organic molecules or transformed them into more easily biodegradable substances.[44] This property led to an excellent COD removal efficiency.

(ii) Indirect oxidation: With the chloride ion concentration, the ability of electric conduction could be improved and the passivation of the electrode could be relieved. Moreover, chloride ions also competed with organic matter to be oxidized at the anode.[45] During the electrochemical process, the chloride ion (Cl$^-$) would be discharged at the anode to generate dissolved gas chlorine (Cl$_2$), then the Cl$_2$ could be chemically converted to hypochlorite ion (OCl$^-$). This was the reason for

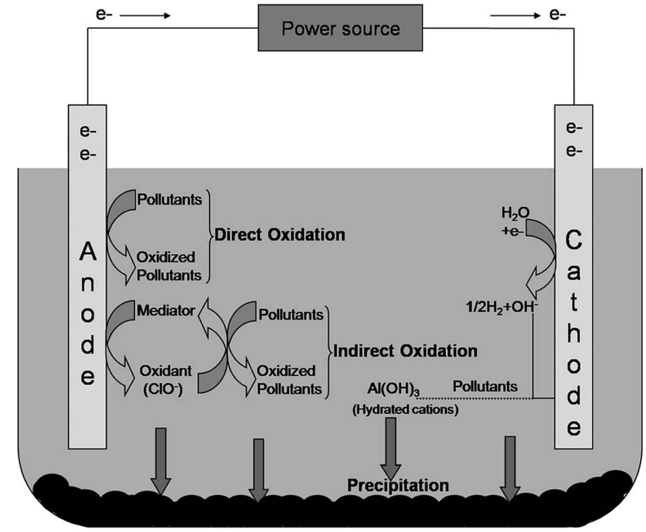

Fig. 6 The reaction mechanism responsible for the removal of pollutants.

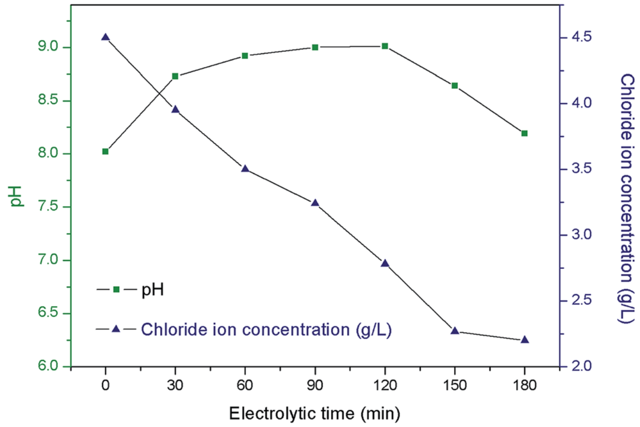

Fig. 7 pH and chloride ion concentration variations in the process of electrolysis.

that the chloride ion concentration in the solution had been decreased, until reached a constant value. The possible reactions occurring were listed below:

$$2Cl^- - 2e^- \rightarrow Cl_2 \tag{6}$$

$$Cl_2 + H_2O \rightarrow HOCl + H^+ + Cl^- \tag{7}$$

$$HOCl \rightarrow H^+ + OCl^- \tag{8}$$

The sum of the three species: Cl^-, Cl_2, and ClO^- were termed free chlorine. In the normal pH range of pond water (6–7.5), ClO^- was the major component of free chlorine. In turn, as "active chlorine" possessing a high stability and oxidation capacity, OCl^- could accelerate the mineralization of organics effectively. In this case, NH_3–N in the leachate could be also removed preferentially through the mechanism similar to "breakpoint reactions":[46]

$$HOCl + NH_4^+ \rightarrow NH_2Cl + H_2O + H^+ \tag{9}$$

$$HOCl + NH_2Cl \rightarrow NHCl_2 + H_2O \tag{10}$$

$$NHCl_2 + H_2O \rightarrow NOH + 2H^+ + 2Cl^- \tag{11}$$

$$NHCl_2 + NOH \rightarrow N_2 + HOCl + H^+ + Cl^- \tag{12}$$

On the whole, both direct and indirect oxidations were involved in COD and NH_3–N removal. And COD removal by direct oxidation occurred at a higher rate than that of NH_3–N, while indirect oxidation preferred removal of NH_3–N than that of COD.

In cathode: Picard *et al.*[47] showed that there was a chemical attack on the aluminum cathode by hydroxide ions generated during water reduction eqn (13), leading to increase of the pH essentially. It was well established that the dissolution occurred through the intermediate of an oxide/hydroxide film,[18] which was formed spontaneously and existed on the surface of aluminium. As expressed by eqn (14) and (15), aluminum cation along with OH^- ion formed a hydroxide of a network structure, large surface area and high absorption. As colloid coagulant, mainly at pH values in the range of 6.0–7.0, they promoted the generation of sweep flocs inside the treated wastewater, whose enmeshment made pollutants removed. Once the colloidal matter was destabilized, it could be separated from the wastewater. In addition to COD and NH_3–N removal, this mechanism played a key role in removal of heavy metals from landfill leachate. It was found that the corrosion rate of aluminium increased during cathodic polarization, being coupled with the hydrogen evolution arising from the attack by hydroxide ions near the electrode surface. And the amount of hydroxide generated in the process was strongly influenced by the pH and the current density. Aluminum had a very low corrosion rate in neutral solutions due to the formation of an insoluble passive film, but the rapid cathodic aluminum dissolution could be observed in low or high pH electrolytes, which was in a good agreement with the results of Moon and Pyun.[17,48] It was also noted that the corrosion rate increases with increasing applied cathodic current density. These could justify the important contribution of the chemical dissolution of aluminum in the cathode to the COD, NH_3–N and heavy metals removal.

$$2H_2O + e^- = H_2 + 2OH^- \tag{13}$$

$$Al + 3OH^- = Al(OH)_3 \tag{14}$$

$$Al(OH)_3 + OH^- = Al(OH)_4^-. \tag{15}$$

3.4 Economic evaluation

The technical feasibility of the electrochemical process was usually evaluated in terms of the percentage removal of pollutants reached, while the economic feasibility was determined by the energy consumption. Typical costs in landfill leachate treatment with the combination of electrooxidation–coagulation processes were the expenditure on energy consumption, mass loss of electrodes and the chemical addition.[22] Among them, chemical addition was only used for the purpose of initial pH adjustment and additional electrolyte, whose dosage was reasonably few. Thus, it was out of the scope of the present work.

In Fig. 8, it reported the variation of specific energy consumption, as function of COD and NH_3–N removal, in the optimum operating condition found previously. For low current density, the specific energy consumption increases almost linearly, while E_{EM}(COD) increased slowly and E_{EM}(NH_3–N) increased sharply for high current density. This behaviour could be probably explained by the decrease of organic content or the formation of more refractory product in the solution. Under the optimum conditions, the electrochemical treatment for 1 kg COD and 1 kg NH_3–N in landfill leachate required the power consumption of 61.59 kW h and 106.91 kW h respectively, which was close to other studies.[2] Additionally, the mass loss of an aluminum electrode for a liter of leachate being treated was 0.46 g.

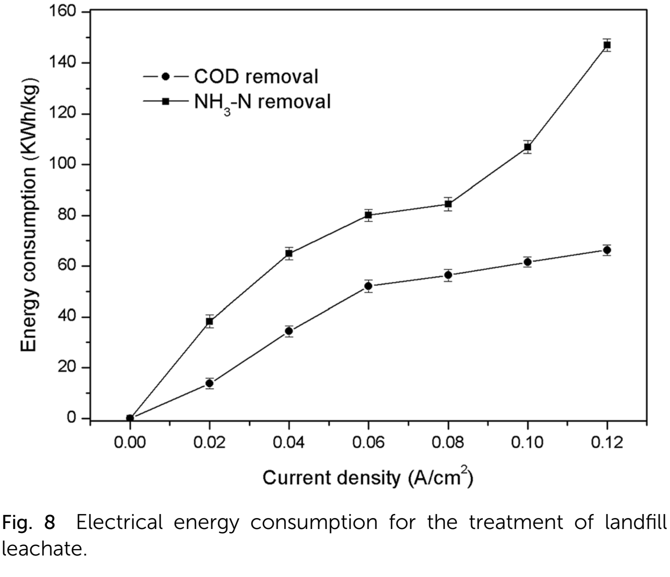

Fig. 8 Electrical energy consumption for the treatment of landfill leachate.

4. Conclusions

This study demonstrated that when the combination of Ti/RuO_2–IrO_2 and Al electrode, they could achieve a significant synergy. The process was found to had an excellent removal performance for COD, NH_3–N, colour and heavy metals in landfill leachate, and could effectively reduce the contaminant loading of these effluents and enhance biodegradability, improved from a BOD_5/COD ratio of 0.12 to 0.38.

Observed the effects of variables using RSM, an optimal operating condition were found to be: current density of 0.1 A cm^{-2}, pH of 6.37, the chloride ion concentration of 6.5 g L^{-1}, electrolysis time 150 min and electrode gap 5 cm, respectively. Under these conditions, the removal rates of COD and NH_3–N were found to be 83.93% and 100%, respectively, which were consistent with the overlay plot results. Therefore, RSM could be effectively adopted to optimize the operating multifactor in complex electrochemical process. In addition, the behaviors of COD, NH_3–N and heavy metals removal were investigated. The predominant mechanisms included oxidation, coagulation and precipitation, confirmed by GC-MS, ESEM/EDS and FTIR analyses.

In most cases, a single technology was insufficient to achieve acceptable levels of pollution decrease. Thus, the further development of integrated different techniques is in demand for taking into account a technically and economically feasible option. The experiment proved that this method was convenient and efficient for primary or deep treatment of wastewater. Coupling with a biological unit will be a promising way, which can obtain an effluent for its reuse or discharge to natural water sources.

Acknowledgements

This study was supported by National Natural Science Foundation of China (51578223, 51378189 and 51521006).

References

1 R. Cossu, A. M. Polcaro, M. C. Lavagnolo, M. Mascia, S. Palmas and F. Renoldi, *Environ. Sci. Technol.*, 1998, **32**, 3570–3573.

2 M. Panizza and C. A. Martinez-Huitle, *Chemosphere*, 2013, **90**, 1455–1460.

3 E. Turro, A. Giannis, R. Cossu, E. Gidarakos, D. Mantzavinos and A. Katsaounis, *J. Hazard. Mater.*, 2012, **207**, 73–78.

4 J. Wu, H. Zhang, N. Oturan, Y. Wang, L. Chen and M. A. Oturan, *Chemosphere*, 2012, **87**, 614–620.

5 F. F. Cai, Z. H. Yang, H. Jing, G. M. Zeng, L. K. Wang and Y. Jian, *J. Hazard. Mater.*, 2014, **275**, 63–71.

6 F. C. Moreira, J. Soler, A. Fonseca, I. Saraiva, R. A. R. Boaventura, E. Brillas and V. J. P. Vilar, *Water Res.*, 2015, **81**, 375–387.

7 A. Anglada, A. Urtiaga, I. Ortiz, D. Mantzavinos and E. Diamadopoulos, *Water Res.*, 2011, **45**, 828–838.

8 A. Coors, P. D. Jones, J. P. Giesy and H. T. Ratte, *Environ. Sci. Technol.*, 2003, **37**, 3430–3434.

9 J. L. de Morais and P. P. Zamora, *J. Hazard. Mater.*, 2005, **123**, 181–186.

10 H. Zhang, X. Ran, X. Wu and D. Zhang, *J. Hazard. Mater.*, 2011, **188**, 261–268.

11 A. Cabeza, A. Urtiaga, M. J. Rivero and I. Ortiz, *J. Hazard. Mater.*, 2007, **144**, 715–719.

12 F. C. Moreira, J. Soler, A. Fonseca, I. Saraiva, R. A. R. Boaventura, E. Brillas and V. J. P. Vilar, *Appl. Catal., B*, 2016, **182**, 161–171.

13 P. Marco and C. Giacomo, *Chem. Rev.*, 2009, **109**, 6570–6631.

14 N. Oturan, E. D. van Hullebusch, H. Zhang, L. Mazeas, H. Budzinski, M. K. Le and M. A. Oturan, *Environ. Sci. Technol.*, 2015, **49**, 12187–12196.

15 A. Fernandes, D. Santos, M. J. Pacheco, L. Ciriaco and A. Lopes, *Appl. Catal., B*, 2014, **148**, 288–294.

16 E. Turro, A. Giannis, R. Cossu, E. Gidarakos, D. Mantzavinos and A. Katsaounis, *J. Hazard. Mater.*, 2011, **190**, 460–465.

17 S. M. Moon and S. I. Pyun, *Corros. Sci.*, 1997, **39**, 399–408.

18 M. Mokaddem, P. Volovitch, F. Rechou, R. Oltra and K. Ogle, *Electrochim. Acta*, 2010, **55**, 3779–3786.

19 W. G. Walter, *Am. J. Public Health Nation's Health*, 1961, 940.

20 J. Wu, H. Zhang, N. Oturan, Y. Wang, L. Chen and M. A. Oturan, *Chemosphere*, 2012, **87**, 614–620.

21 X. Mo, Z. H. Yang, H. Y. Xu, G. M. Zeng, J. Huang, X. Yang, P. P. Song and L. K. Wang, *J. Hazard. Mater.*, 2015, **286**, 493–502.

22 T. F. C. V. Silva, A. Fonseca, I. Saraiva, R. A. R. Boaventura and V. J. P. Vilar, *Chem. Eng. J.*, 2016, **283**, 76–88.

23 B. Cercado-Quezada, M.-L. Delia and A. Bergel, *Electrochem. Commun.*, 2011, **13**, 440–443.

24 H. Wang, S. Yuan, J. Zhan, Y. Wang, G. Yu, S. Deng, J. Huang and B. Wang, *Water Res.*, 2015, **80**, 20–29.

25 L. R. Czarnetzki and L. J. J. Janssen, *J. Appl. Electrochem.*, 1992, **22**, 315–324.

26 G. Mouedhen, M. Feki, M. D. Petris-Wery and H. F. Ayedi, *J. Hazard. Mater.*, 2009, **168**, 983–991.

27 Z. Zaroual, H. Chaair, A. H. Essadki, K. E. Ass and M. Azzi, *Chem. Eng. J.*, 2009, **148**, 488–495.

28 L. C. Chiang, J. E. Chang and T. C. Wen, *Water Res.*, 1995, **29**, 671–678.

29 F. Feki, F. Aloui, M. Feki and S. Sayadi, *Chemosphere*, 2009, **75**, 256–260.

30 D. Yang and J. D. Englehardt, *Waste Manag.*, 2007, **27**, 380–388.

31 P. B. Moraes and R. Bertazzoli, *Chemosphere*, 2005, **58**, 41–46.

32 G. Del Moro, L. Prieto-Rodríguez, M. De Sanctis, C. Di Iaconi, S. Malato and G. Mascolo, *Chem. Eng. J.*, 2016, **288**, 87–98.

33 H. Zhang, Y. Li, X. Wu, Y. Zhang and D. Zhang, *Waste Manag.*, 2010, **30**, 2096–2102.

34 J. E. Silveira, J. A. Zazo, G. Pliego, E. D. Bidóia and P. B. Moraes, *Environ. Sci. Pollut. Res. Int.*, 2014, **22**, 5831–5841.

35 E. Turro, A. Giannis, R. Cossu, E. Gidarakos, D. Mantzavinos and A. Katsaounis, *J. Hazard. Mater.*, 2011, **190**, 460–465.

36 N. Fan, Z. Li, L. Zhao, N. Wu and T. Zhou, *Chem. Eng. J.*, 2013, **214**, 83–90.

37 M. Li, C. Feng, Z. Zhang and N. Sugiura, *Electrochim. Acta*, 2009, **54**, 4600–4606.

38 A. A. Bukhari, *Bioresour. Technol.*, 2008, **99**, 914–921.

39 H. Zhang, X. Ran, X. Wu and D. Zhang, *J. Hazard. Mater.*, 2011, **188**, 261–268.

40 Y. Lei, Z. Shen, R. Huang and W. Wang, *Water Res.*, 2007, **41**, 2417–2426.

41 S. Aoudj, A. Khelifa, N. Drouiche, R. Belkada and D. Miroud, *Chem. Eng. J.*, 2015, **267**, 153–162.

42 H. Zoellig, A. Remmele, C. Fritzsche, E. Morgenroth and K. M. Udert, *Environ. Sci. Technol.*, 2015, **49**, 11062–11069.

43 J. A. Gomes, P. Daida, M. Kesmez, M. Weir, H. Moreno, J. R. Parga, G. Irwin, H. McWhinney, T. Grady, E. Peterson and D. L. Cocke, *J. Hazard. Mater.*, 2007, **139**, 220–231.

44 A. Fernandes, M. J. Pacheco, L. Ciríaco and A. Lopes, *Appl. Catal., B*, 2015, **176–177**, 183–200.

45 A. Angela, U. Ane and O. Inmaculada, *Environ. Sci. Technol.*, 2009, **43**, 2035–2040.

46 Y. Gendel and O. Lahav, *Electrochim. Acta*, 2012, **63**, 209–219.

47 T. Picard, G. Cathalifaud-Feuillade, M. Mazet and C. Vandensteendam, *J. Environ. Monit.*, 2000, **2**, 77–80.

48 S. O. Klemm, J. P. Kollender and A. Walter Hassel, *Corros. Sci.*, 2011, **53**, 1–6.